



**HAL**  
open science

## Electronic Structure of Leached Al-Cu-Fe Quasicrystals used as Catalysts

Esther Belin-Ferré, Marie-Francoise Fontaine, Jean Thirion, Satoshi Kameoka,  
a Peter Tsai, Jean-Marie Dubois

► **To cite this version:**

Esther Belin-Ferré, Marie-Francoise Fontaine, Jean Thirion, Satoshi Kameoka, a Peter Tsai, et al..  
Electronic Structure of Leached Al-Cu-Fe Quasicrystals used as Catalysts. Philosophical Magazine,  
2005, 86 (03-05), pp.687-692. 10.1080/14786430500318902 . hal-00513613

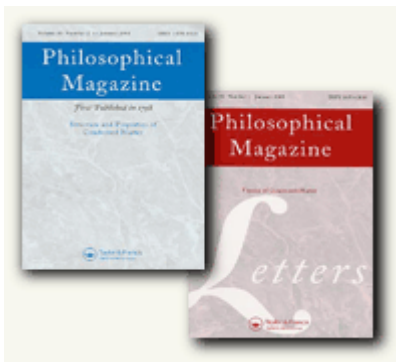
**HAL Id: hal-00513613**

**<https://hal.science/hal-00513613>**

Submitted on 1 Sep 2010

**HAL** is a multi-disciplinary open access archive for the deposit and dissemination of scientific research documents, whether they are published or not. The documents may come from teaching and research institutions in France or abroad, or from public or private research centers.

L'archive ouverte pluridisciplinaire **HAL**, est destinée au dépôt et à la diffusion de documents scientifiques de niveau recherche, publiés ou non, émanant des établissements d'enseignement et de recherche français ou étrangers, des laboratoires publics ou privés.



**Electronic Structure of Leached Al-Cu-Fe Quasicrystals used as Catalytis**

Journal:	<i>Philosophical Magazine &amp; Philosophical Magazine Letters</i>
Manuscript ID:	TPHM-05-May-0204.R2
Journal Selection:	Philosophical Magazine
Date Submitted by the Author:	17-Aug-2005
Complete List of Authors:	Belin-Ferré, Esther; Laboratoire de Chimie Physique Matière et Rayonnement, Unité Mixte de Recherche Fontaine, Marie-Francoise; Laboratoire de Chimie Physique Matière et Rayonnement Thirion, Jean; Laboratoire de Chimie Physique Matière et Rayonnement Kameoka, Satoshi; Tohoku University Tsai, A; Tohoku University, National Institute for Materials Science Dubois, Jean-Marie; Ecole des Mines de Nancy, Laboratoire de Science et Génie des Matériaux et de Métallurgie
Keywords:	quasicrystals, electronic structure, catalysts
Keywords (user supplied):	X-ray emission spectroscopy



## Electronic structure of leached Al-Cu-Fe quasicrystals used as catalysts

E. BELIN-FERRÉ†\*, M-F. FONTAINE†, J. THIRION†,  
S. KAMEOKA‡, A.P. TSAI‡ and J.M. DUBOIS††

†Laboratoire de Chimie Physique Matière et Rayonnement ~~Unité Mixte de Recherche 7614~~, 11 rue P.  
et M. Curie,  
75231 Paris Cedex 05, France

‡Institute for Multidisciplinary Research for Advanced Materials, 2-1-1 Katahira, Aoba-ku,  
Sendai 980-8577, Japan

††Laboratoire de Science et Génie des Matériaux et de Métallurgie, Ecole des Mines, Parc de Saurupt,  
54042 Nancy, France

**Abstract.** We used X-ray emission spectroscopy to investigate the electronic structure of various catalysts obtained by leaching a quasicrystalline Al-Cu-Fe compound in 5%Na<sub>2</sub>CO<sub>3</sub> aqueous solution. The study of Al states confirmed that ~~upon leaching~~ Al is almost totally oxidised in the catalysts. Fe is not as much oxidised probably because it is embedded in Cu-Al<sub>2</sub>O<sub>3</sub> grains. Cu is only partly oxidised. However, ~~from our data~~ it is not excluded that the catalytic activity could be due to a size effect that prevents the formation of a band as in metallic Cu, and gives to the electronic structure an atomic-like character. New measurements should be done from fresh specimens in order to ~~make sure that no~~ **avoid** further oxidation interferes with the Cu spectral distributions ~~in the catalysts~~.

Keywords: quasicrystals, catalysts, electronic structure, x-ray emission spectroscopy

### Introduction

Al-Cu-Fe quasicrystalline compounds leached in a 5%Na<sub>2</sub>CO<sub>3</sub> aqueous solution exhibit high performance catalytic properties for steam reforming of methanol [1, 2]. Annealing in air at 600°C enhances the catalytic activity, ~~whereas~~ it is decreased by further annealing in H<sub>2</sub> atmosphere. To investigate which is the reason for this behaviour, we studied the electronic structure of such catalysts using X-ray emission spectroscopy (XES) ~~This technique which probes partial electronic distributions~~ **densities of states (DOS)** around each chemical species in a sample. ~~Here, we have analysed Al 3p, Al 3s,d, Cu 3d and Fe 3d states in various specimens as indicated in the next section~~ **For details on XES and the electronic structure of quasicrystals see reference [3].**

### Experimentals

We have studied ~~the following~~ **several** samples: (i) sample labelled A is a quasicrystalline Al-Cu-Fe Al<sub>63</sub>Cu<sub>25</sub>Fe<sub>12</sub> powder (**grains < 150µm**) annealed for 24 hours at 800°C ~~for homogenisation purposes~~, (ii) sample B is powder A leached in a 5%Na<sub>2</sub>CO<sub>3</sub> aqueous solution ~~and washed to remove all alkali traces~~, (iii) sample C is powder B, annealed for 4 hours in air at 600°C, (iiii) sample D is powder C, annealed at 600°C for 4 hours in H<sub>2</sub> atmosphere. The ~~Cu Kα~~ x-ray diffraction patterns are dominated by the peaks of the quasicrystalline compound, but also display for samples B, C and D diffraction peaks of Al<sub>2</sub>O<sub>3</sub>, CuO and a β-phase. Cu particles of about 10 nm in size were found to be dispersed at the surface of the catalysts. ~~Pure metals, oxides (Al<sub>2</sub>O<sub>3</sub> and Fe<sub>3</sub>O<sub>4</sub>) and spinel compounds (CuAl<sub>2</sub>O<sub>4</sub> and CuFe<sub>2</sub>O<sub>4</sub>) were also analysed for comparison purposes~~

~~The XES spectral curves were recorded in vacuum spectrometers fitted with a crystalline slab for Al~~

3p, Cu 3d and Fe 3d states, respectively, or a grating for Al 3s,d states. The powders stuck onto water cooled holders, were irradiated by electrons of energies allowing to excite the x ray transitions: valence band (VB)  $\rightarrow$  Al 2p<sub>3/2</sub>, VB  $\rightarrow$  Al 1s, VB  $\rightarrow$  Cu 2p<sub>3/2</sub> and VB  $\rightarrow$  Fe 2p<sub>3/2</sub> levels to probe Al 3s-d, Al 3p, Cu 3d and Fe 3d states, respectively. The energy resolution was about 0.4 eV for Al spectra and 0.5 eV for Cu and Fe spectra. The XES technique does not display absolute density of states values. Hence each spectral curve is normalised to its own maximum intensity and it is presented in the x ray transition energy scale.

The XES spectral curves probe Al3s-d, Al3p, Cu3d and Fe3d states, respectively owing to the transitions: valence band (VB)  $\rightarrow$  Al2p<sub>3/2</sub>, VB  $\rightarrow$  Al1s, VB  $\rightarrow$  Cu2p<sub>3/2</sub> and VB  $\rightarrow$  Fe2p<sub>3/2</sub> levels. The energy resolution was about 0.4 eV for Al spectra and 0.5 eV for Cu and Fe spectra and the experimental accuracy between 0.1-0.2 eV. As the XES technique does not provide absolute DOS values, each spectral curve is normalised to its own maximum intensity in the x-ray transition energy scale. Pure metals, Al<sub>2</sub>O<sub>3</sub>, Fe<sub>3</sub>O<sub>4</sub> and spinel compounds (CuAl<sub>2</sub>O<sub>4</sub> and CuFe<sub>2</sub>O<sub>4</sub>) were also analysed for comparison purposes.

## Results

Figure 1 shows the results for Al 3s-d states in the left side panel and for Al 3p states in the right side panel. In both panels, the two full and dashed curves at the same lower ordinate correspond to samples A and Al<sub>2</sub>O<sub>3</sub>, respectively. From bottom to top, the lines with triangles, diamonds and dots refer to samples B, C and D, respectively. In the right side panel, the upper curve corresponds to spinel CuAl<sub>2</sub>O<sub>4</sub>.

**Figure 1 shows the curves for Al3s-d and Al3p states.**

The shapes of the Al3s-d curves of B, C and D samples (left side panel) are very similar and depart from the curve of sample A. They look like the curve for Al in Al<sub>2</sub>O<sub>3</sub>. In addition they but display a faint feature around 71 eV in the energy range of a maximum of the curve of sample A. Clearly, samples B, C and D are highly oxidised and show traces of non-oxidised material. For sample B, the peak in the range 67-68 eV is broader than in Al<sub>2</sub>O<sub>3</sub> and bent towards low transition energies due to overlap from oxidised and non-oxidised contributions. The traces of non-oxidised material These are less important for samples C and D than for sample B. Yet, for both C and D specimens, the contributions due to non-oxidised material also broaden and slightly shift the peak in the range 67-68 eV towards low energies as compared to pure alumina. The peak at 64 eV is unchanged in all these samples within the experimental accuracy. In this energy range, the intensity of the curve for sample A, not oxidised, is rapidly decreasing.

The shapes of the Al3p curves for samples B, C and D (right side panel), also significantly depart from the curve of sample A and are similar to the curve that of alumina. Hence, again the samples are highly oxidised. Still, the wing on B, C and D curves around 1558-1560 eV, the energy range where the intensity increases up to of the maximum in curve A, is slightly less hollow than in for Al<sub>2</sub>O<sub>3</sub>. Accordingly, there exists some contribution from non-oxidised material in this energy range. The curves of spinel CuAl<sub>2</sub>O<sub>4</sub> is similar to that of and Al<sub>2</sub>O<sub>3</sub> are analogous. However, the peak at 1539 eV is of higher intensity in the spinel than in oxide; this peak arises from a transition from the VB towards O 2s states hybridised to Al 3p states. The difference in intensity of this peak between the two samples gives an indication that their electronic structures although similar, are not identical. **The peak at 1539 eV due to a transition from VB hybridised (O2s - Al3p) states  $\rightarrow$  Al 1s, is of higher intensity in the spinel than in oxide. Hence their electronic structures although similar, are not identical.**

At this point, it appears that Thus, Al whatever the specimen, except in powder A, is highly oxidised. In bulk fcc Al, the depths sampled by the excitation beam for investigating Al3s-d and Al3p states respectively, are of the order of 0.3 to 0.5  $\mu$ m and surface contribution, especially contribution of the oxide, amounts to at most a few per cent of the total signal. For powders, it is not straightforward to quantify precisely the importance of oxidation. Since powder grains represent a large surface

contribution to XES data, it makes sense to assume that the oxide contribution dominates the spectra. Actually, it could be estimated from the curves to be of the order of 90% the total signal.

Figure 2 displays the Cu 3d distribution curves in both panels. In the left side panel, the bottom curves refer to sample A (full line) and pure Cu (dashed line); from bottom to top, one finds the curves of samples B (triangles), C (diamonds) and D (dots). The vertical dashed line marks the energy position of the maximum for curve A. The right side panel shows the curve of sample D and that of spinel  $\text{CuFe}_2\text{O}_4$ . Figure 2 displays the Cu3d distribution curves in the various samples. Within experimental accuracy, the curves of spinels  $\text{CuFe}_2\text{O}_4$  and  $\text{CuAl}_2\text{O}_4$  are identical.

In our experimental conditions, the bulk Cu sampled depth is approximately 17 nm. Accordingly, one expects that the whole of Cu grains are probed in the catalysts during XES measurements.

The shape of curve A is reminiscent of that of pure Cu, but narrower due to the alloying effect [3]. The curves of the catalysts exhibit faint satellites at the same energies as in  $\text{Cu}_2\text{O}$  [4] for (sample B) or and as in both  $\text{Cu}_2\text{O}$  and  $\text{CuO}$  [4] for (sample C). The shape of curve D is more like that of  $\text{CuO}$  [4] (Insert in Fig. 2 right panel) with a clear satellite around 935 eV. In the spinels no satellite is observed (fig. 3 right side panel) which stresses a different electronic structure than in oxides. Because of the satellites, for comparing the full widths at half maximum intensity of the curves (FWHM), one has to consider the low energy part of the spectral distribution and its symmetric with respect to the position of the maximum. The corresponding values are given in Values are in Table 1 together with the energies of the maxima of the curves and the satellites. The data for  $\text{CuO}$  and  $\text{Cu}_2\text{O}$  are obtained from reference 3. The data of reference 4 are obtained from the same experimental setup.

Table 1

Sample	Max Cu 3d $\pm 0.15$ eV	Energy of Satellites $\pm 0.2$ eV	FWHM $\pm 0.1$ eV $\pm 0.2$ eV
Cu	930.10	932.8 935.7	3.0
$\text{CuO}$	929.30	931.8 934.7	2.0
$\text{Cu}_2\text{O}$	929.70	931.2	2.0
$\text{CuAl}_2\text{O}_4$ (spinel)	930.40		2.0
$\text{CuFe}_2\text{O}_4$ (spinel)	930.40		2.0
Quasicrystal : sample A	929.50	931.5 934.4	2.0
Leached : sample B	929.50	931.2 934.4	2.0
Leached+annealed : sample C	929.60	931.2 934.6	2.0
Leached+annealed+ $\text{H}_2$ : sample D	929.50	928.8 931.6 934.6	2.6

Within our experimental precision, except for fcc Cu and sample D, the FWHM of the curves are the same, and the maxima of the curves of the three catalysts are found at intermediate energies between the ones for the two oxides. They differ for the spinels. The maxima of the curves of the three catalysts differ from the spinels and are at energies intermediate between those for the two oxides. From the x-ray diffraction pattern show  $\text{CuO}$  peaks, should contribute to the spectra especially in sample C. The FWHM are the same in catalysts B and C and in oxides. Because the maxima are at the same energy value one may expect that the oxide contribution dominates the spectra of these

catalysts and may hidden any other specificity. Thus one may expect that the oxide contribution is significant to the spectra of these catalysts and may hide other specificities.

In contrast, the curve of sample D is wider than for the others. In addition, this curve It shows one marked feature at  $929.1 \pm 0.2$  eV, namely close to the value for CuO. One explanation is that the curve of sample D results from the addition of a CuO contribution to the genuine distribution due to of catalyst D. Actually, the intensities of the CuO peaks in the diffraction pattern of sample D are much lower than in sample C. Actually, the CuO peaks in the diffraction pattern of sample D are of lower intensity than in sample C. Here, we must underline that **Note that** the catalysts were kept in air. Because they are not reactive in the same way, oxidation upon ageing may have taken place and differ from one sample to the other (the catalytic power of sample D against methanol reforming is slightly lower than that of sample C).

Another change of slope is seen at about  $928.5 \pm 0.2$  eV on the D spectral curve (Fig.2 right panel). Hence, this curve shows 3 features. It is known that in Ni nano-sized metallic particles, the 3d band, d is no longer metallic-like, but shows 5 features which are ascribed to the 5 d individual orbitals [5]. A similar behaviour may occur in the Cu catalysts that are less than 10 nm in size but this effect may be hidden because of oxidation.

At this stage, It is difficult to ascertain whether partial oxidation or size effect are responsible for the shape of the spectral curves of the catalytic samples. We ignore whether the nanometric Cu particles have an "atomic-like" behaviour that could be responsible for their catalytic properties. New experiments are under way, using fresh catalysts kept in argon atmosphere to avoid ageing in air and getting better insight into their genuine electronic structure

Figure 3 displays the Fe3d curves in the catalysts, powder A, pure bcc Fe, and also oxide Fe<sub>3</sub>O<sub>4</sub> and spinel CuFe<sub>2</sub>O<sub>4</sub>. **Many more scans than for sample A were required by all catalysts to achieve equivalent background-to-signal ratio.** For all catalysts, to obtain an equivalent background-to-signal ratio, the measurements required many more scans than for sample A. To interpret this observation, we suggest that Fe atoms are embedded inside Cu-Al<sub>2</sub>O<sub>3</sub> grains. This is supported by the fact that the x-ray diffraction patterns show no contribution due to Fe.

Table 2 collects the data corresponding to these measurements the energy values of the maximum of the L $\alpha$  band (VB $\rightarrow$ Fe2p<sub>3/2</sub>), the FWHM, the ratio between L $\alpha$  and L $\beta$  peaks (this transition L $\beta$  corresponds to VB $\rightarrow$ Fe2p<sub>1/2</sub>) and the energy distance between the two L $\alpha$  and L $\beta$  sub-bands.

Table 2

Sample	Max L $\alpha$ $\pm 0.15$ eV	FWHM $\pm 0.1$ eV $\pm 0.2$ eV	L $\alpha$ /L $\beta$ ratio $\pm 0.2$	L $\beta$ -L $\alpha$ $\pm 0.2$ eV
Fe	704.95	5.1	2.1	12.4
Quasicrystal : sample A	706.54	4.4	3.3	13.0
Leached : sample B	706.78	5.0	2.5	11.4
Leached+annealed : sample C	707.56	5.4	2.3	11.3
Leached+annealed+H <sub>2</sub> : sample D	707.32	5.4	2.2	11.6
Fe <sub>3</sub> O <sub>4</sub>	705.40	5.2	2.1	12.0
CuFe <sub>2</sub> O <sub>4</sub> (spinel)	706.50	5.4	1.9	11.4

The values for samples A, B, C and D differ from the reference compounds, the maxima are shifted opposite to the values of the pure metal. Whereas for compound A the position is quite close to that of Fe in  $\text{CuFe}_2\text{O}_4$  spinel, this is no longer true for the other samples. The value of the  $L\alpha/L\beta$  ratio is completely different in compound A from the ones for pure Fe, spinel or oxide. The trend shown by the catalysts is to tend towards the values for the spinel. In other words, the electronic structure in the catalysts is completely different from that in bcc Fe or  $\text{Fe}_3\text{O}_4$ , but could be similar to that in  $\text{CuFe}_2\text{O}_4$ .

**The values for samples A, B, C and D differ from the reference compounds: whereas for compound A the position is quite close to that of Fe in spinel  $\text{CuFe}_2\text{O}_4$ , this is no longer true for the other samples. The value of the  $L\alpha/L\beta$  ratio is completely different in compound A from the values for pure Fe, spinel or oxide. The electronic structure of the catalysts differs from that in bcc Fe or  $\text{Fe}_3\text{O}_4$ , the Fe oxidation number tends towards that in  $\text{CuFe}_2\text{O}_4$ .**

The spectral curves of catalysts D and C display a marked feature at the energy of the maximum in the oxide  $\text{Fe}_3\text{O}_4$  less pronounced for sample C. Sample C also exhibits such a shoulder but less pronounced. As a result, there is a slight broadening of the curves with respect to sample B as seen from the FWHM values. **Note that** oxidation may occur upon ageing of the samples during the thermal treatments of the samples or, since there is no visible Fe oxide contribution in the x-ray diffraction pattern of the catalysts, it may depend.

## Conclusion

Our XES study of Al states has confirmed that Al is oxidised to at least about 90% in the catalysts. Fe is not as much oxidised, probably because it is embedded in  $\text{Cu-Al}_2\text{O}_3$  grains. For Cu, it cannot be excluded from our data that the catalytic activity of samples B, C and D arises from a size effect that prevents the formation of an electron band and gives an "atomic-like" character to the electronic structure. To ascertain this interpretation, measurements must be repeated with catalytic samples kept in an inert atmosphere in order to make sure that no further oxidation modifies their Cu spectral distributions. **to avoid further oxidation modifies their spectral distributions.**

## References

- [1] A. P. Tsai and M. Yoshimura *Applied Catalysis A* **214** 237 (2001).
- [2] S. Kameoka, T. Tanabe and A. P. Tsai *Catalysis Today* **93-95** 23 (2004).
- [3] E. Belin-Ferré *J. of Phys. Condensed Matter* **14** R789-R817 (2002).
- [4] C. Bonnelle *Annales de Physique* **14ème serie** 1 1 (1966).
- [5] D. Fargues, F. Vergand, E. Belin, C. Bonnelle, D. Olivier, L. Bonneviot and M. Che *Surface Science*, **106** 239 (1981).

### Figure captions

Figure 1. From bottom to top: Al 3s-d (left side panel) and Al 3p (right side panel) distribution curves in sample A (full line) and  $\text{Al}_2\text{O}_3$  (dashed line), samples B (triangles), C (diamonds) and D (dots). In the right side panel the upper full line refers to  $\text{CuAl}_2\text{O}_4$  spinel

Figure 2. Left side panel: from bottom to top, Cu 3d distribution curves in sample A (full line) and pure fcc Cu (dashed line), samples B (triangles), C (diamonds) and D (dots). Right side panel: Cu 3d spectral curve in sample D (full line) and spinel  $\text{CuFe}_2\text{O}_4$  (diamonds). The bars labelled 1, 2 and 3 show the energies of the maxima of CuO,  $\text{Cu}_2\text{O}$  and Cu distributions, respectively. In the insert, from bottom to top, Cu 3d distribution curves in CuO and  $\text{Cu}_2\text{O}$ , respectively [4].

Figure 3. Fe 3d distribution curves in bcc Fe (dashed lower curve),  $\text{Fe}_3\text{O}_4$  (thin lower line) and spinel  $\text{CuFe}_2\text{O}_4$  (thick lower line). At upper coordinates, from bottom to top, are shown the same spectra in samples A (no symbol), B (triangles), C (diamonds) and D (dots). From left to right, the vertical lines mark the maximum of the Fe  $L\alpha$  distribution (see text) in the pure metal, oxide and spinel (dashed line).

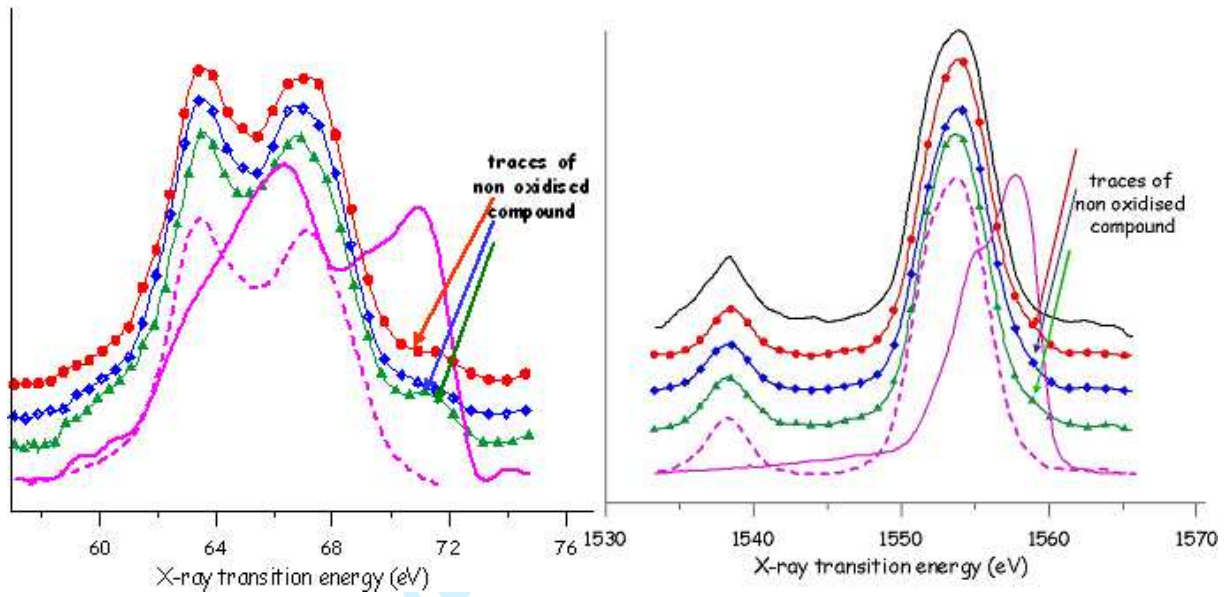
### Table captions

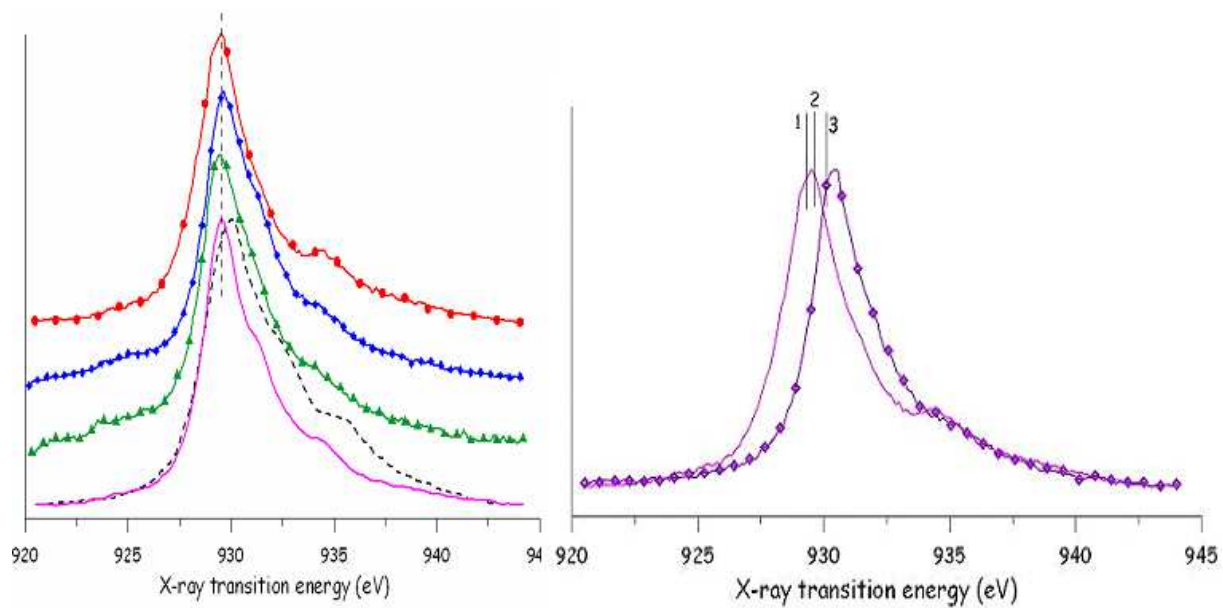
Table 1. FWHM and energies of the features of Cu 3d spectral curves

Table 2. Energies values of the features of the Fe 3d spectral curves

1  
2  
3  
4  
5  
6  
7  
8  
9  
10  
11  
12  
13  
14  
15  
16  
17  
18  
19  
20  
21  
22  
23  
24  
25  
26  
27  
28  
29  
30  
31  
32  
33  
34  
35  
36  
37  
38  
39  
40  
41  
42  
43  
44  
45  
46  
47  
48  
49  
50  
51  
52  
53  
54  
55  
56  
57  
58  
59  
60

For Peer Review Only





Peer Review Only

1  
2  
3  
4  
5  
6  
7  
8  
9  
10  
11  
12  
13  
14  
15  
16  
17  
18  
19  
20  
21  
22  
23  
24  
25  
26  
27  
28  
29  
30  
31  
32  
33  
34  
35  
36  
37  
38  
39  
40  
41  
42  
43  
44  
45  
46  
47  
48  
49  
50  
51  
52  
53  
54  
55  
56  
57  
58  
59  
60

